BIOLOGY OF REPRODUCTION **62,** 1866–1874 (2000)

Oxidative Phosphorylation-Dependent and -Independent Oxygen Consumption by Individual Preimplantation Mouse Embryos[1]

James R. Trimarchi,[3] Lin Liu,[3,6] D. Marshall Porterfield,[5] Peter J.S. Smith,[4] and David L. Keefe[2,3,5]

Laboratory for Reproductive Medicine,[3] Marine Biological Laboratory, Woods Hole, Massachusetts 02543
BioCurrents Research Center,[4] Marine Biological Laboratory, Woods Hole, Massachusetts 02543
Department of Biological Sciences,[5] University of Missouri-Rolla, Rolla, Missouri 65409
Women and Infants Hospital,[6] Brown University, Providence, Rhode Island 02905

ABSTRACT

The self-referencing electrode technique was employed to noninvasively measure gradients of dissolved oxygen in the medium immediately surrounding developing mouse embryos and, thereby, characterized changes in oxygen consumption and utilization during development. A gradient of depleted oxygen surrounded each embryo and could be detected >50 μm from the embryo. Blastocysts depleted the surrounding medium of 0.6 ± 0.1 μM of oxygen, whereas early cleavage stage embryos depleted the medium of only 0.3 ± 0.1 μM of oxygen, suggesting a twofold increase in oxygen consumption at the blastocyst stage. Mitochondrial oxidative phosphorylation (OXPHOS) accounted for 60–70% of the oxygen consumed by blastocysts, while it accounted for only 30% of the total oxygen consumed by cleavage-stage embryos. The amount of oxygen consumed by non-OXPHOS mechanisms remained relatively constant throughout preimplantation development. By contrast, the amount of oxygen consumed by OXPHOS in blastocysts is greater than that consumed by OXPHOS in cleavage-stage embryos. The amount of oxygen consumed by one-cell embryos was modulated by the absence of pyruvate from the culture medium. Treatment of one-cell embryos and blastocysts with diamide, an agent known to induce cell death in embryos, resulted in a decline in oxygen consumption, such that the medium surrounding dying embryos was not as depleted of oxygen as that surrounding untreated control embryos. Together these results validate the self-referencing electrode technique for analyzing oxygen consumption and utilization by preimplantation embryos and demonstrate that changes in oxygen consumption accompany important physiological events, such as development, response to medium metabolites, or cell death.

INTRODUCTION

The mammalian oocyte contains approximately 100 000 mitochondria [1, 2], each of which harbors DNA (mtDNA) that encodes essential components of oxidative phosphorylation (OXPHOS) machinery [3]. Mitochondrial DNA can be damaged by oxidative stress [4] and a wide variety of mtDNA rearrangements appear in oocytes from infertile women [5]. The heteroplasmy of oocyte mtDNA challenges currently available genetic technology and therefore limits the ability of molecular genetic approaches to predict mitochondrial function. Measurements of oxygen consumption from oocytes and embryos should provide a more direct assay of mitochondrial function and dysfunction.

More than 60 yr have past since the first oxygen measurements were taken from mammalian oocytes or embryos [6–8]. Using a Cartesian diver technique, initial studies demonstrated that groups of blastocysts consumed markedly more oxygen than did groups of cleavage-stage embryos and that changing the concentration of metabolic substrates in culture medium altered the amount of oxygen consumed by embryos [6–11]. Subsequent studies employed a microspectrophotometric technique to analyze spectral shifts in extracellular oxyhemoglobin resulting from oxygen consumption by embryos [12–14]. Stationary solid-state oxygen electrodes also have been employed to measure oxygen consumption from groups of embryos and from individual embryos. Using these electrodes, Overstrom et al. [15] documented, as had Magnusson et al. [12] using spectrophotometric methods, that embryos consuming more oxygen developed to blastocysts and exhibited higher survival rates than those that consumed less oxygen, although these results have not been subsequently confirmed. Also using oxygen electrodes, Benos and Balaban [16] determined that between 50 and 70% of the oxygen consumed by blastocysts was utilized by OXPHOS to generate ATP for the plasma membrane Na/K-ATPase, and Manes and Lai [17] demonstrated that a portion of the total oxygen consumed by embryos was not utilized by mitochondrial OXPHOS, but by other oxygenases. More recently, Houghton et al. [18] developed an ultrafluorescence technique to measure oxygen consumption and expanded upon the relationship between medium metabolites and oxygen consumption by embryos.

It is upon this historical backdrop that we apply a novel technology for assessing oxygen consumption from individual oocytes and embryos. The self-referencing electrode technique [19, 20] allows noninvasive measurements of physiological parameters from individual cells by detecting differences between the composition of the medium immediately surrounding cells relative to that of the bulk medium. The exquisite sensitivity of this methodology arises by moving an electrode between two positions, 10 μm apart. One pole of the electrode oscillation measures the physiological signal near the cell while the other pole of the oscillation measures the physiological signal at a position remote from the cell. By obtaining the difference between the measurements at these two sites, the contribution of electronic drift is reduced and the resultant signal obtained is proportional to the difference in the concentration of the measured parameter at these two positions. This technique has been used to measure oxygen consumption from a variety of cell types [21] and recently was employed to

[1]A portion of this work was supported by grants NIH R21 RR 12718-02 to D.L.K. and P.J.S.S; KO81099 to D.L.K.; and NIH P41 RR01395 to P.J.S.S.
[2]Correspondence: David Keefe, Laboratory for Reproductive Medicine, Lillie Building, Marine Biological Laboratory, 7 MBL Street, Woods Hole, MA 02543. FAX: 508 540 6902; e-mail: dkeefe@wihri.org

Received: 8 November 1999.
First decision: 6 December 1999.
Accepted: 27 January 2000.

ISSN: 0006-3363. http://www.biolreprod.org

characterize the baseline oxygen consumed by developing embryos [22].

Here, we present the application of this technique to investigate the modulation of embryonic oxygen consumption by a number of factors, including; mitochondrial toxins, a metabolic substrate in the culture medium, and a cell death-inducing agent known to evoke changes in mitochondria [23]. To our knowledge, significant levels of mtDNA rearrangements have not been reported in wild-type or genetically engineered mouse oocytes. Therefore, we have employed pharmacological agents to perturb OXPHOS in mouse oocytes and, by this approach, have determined the contribution of mitochondrial OXPHOS-dependent and OXPHOS-independent processes to the total oxygen consumed by individual embryos.

One benefit of the self-referencing electrode technique is that oxygen measurements can be noninvasively obtained from individual embryos and therefore this technology can interface with other single-cell techniques, such as polymerase chain reaction (PCR) of mtDNA deletions [5], metabolite-uptake/lactate-secretion assays [24, 25], mitochondria redistribution dynamics [26], preimplantation genetic diagnosis [27, 28], in vivo protein dynamic studies using green-fluorescent protein (GFP) [29], and fluorescence resonance energy transfer (FRET) [30]. The self-referencing electrode technique also will permit exploration of subtle changes in oxygen consumption that otherwise would be unattainable from groups of asynchronous embryos and may eventually provide a diagnostic tool for assessing the level of mitochondria dysfunction and developmental potential of individual embryos.

MATERIALS AND METHODS

The self-referencing system used to monitor oxygen gradients around embryos was identical to that previously described [19–22]. Briefly, this system was composed of a Zeiss Axiovert 100 TV inverted microscope (Carl Zeiss, Inc., Thornwood, NY) with a modified stage plate to which computer-controlled micromanipulators were affixed (BioCurrents Research Center, MBL, Woods Hole, MA). The microscope rested on a Kinetic Systems Vibraplane vibration-resistant table (Boston, MA) enclosed in a stainless steel insulated chamber. The temperature of the chamber and its contents, including the microscope and manipulators, was maintained at 37°C. Physiological measurements were conducted in 4 ml of HEPES-buffered KSOM (HKSOM) containing reduced $NaHCO_3$ (4 mM) and elevated HEPES (14 mM) absent of an oil overlay and at atmospheric gas pressures. Recordings were obtained from embryos in plastic petri dishes with a coverglass bottom (MatTek Corp., Ashland, MA) that facilitated embryo positional stabilization. Typically, a set of four to six embryos was placed in a dish, and at least three independent recordings were obtained over several minutes from each embryo in a semirandomized order. Approximately 60 min was required to complete the measurements from a set of embryos. We have shown that mouse embryos exposed to these conditions developed to blastocysts and live pups at a frequency similar to control embryos not physiologically examined (unpublished data), and oxygen gradients around embryos were stable throughout the measurement period.

Oxygen-sensitive electrodes (tip diameter of 2–4 μm) were purchased from Diamond General Corp. (Ann Arbor, MI) and used as previously described [21, 22]. A silver/silver chloride reference electrode completed the circuit in solution by way of a 3 mol L^{-1} KCl/3% agar bridge. All electrodes were calibrated in saturated oxygen and saturated nitrogen solutions. During recording, the electrode was oscillated in a square wave parallel to the electrode axis over a distance of 10 μm with a frequency of 0.3 Hz. Initially, the near position of this oscillation was 1.5–2.5 μm from the zona pellucida or plasma membrane in cases where the zona pellucida was removed by brief pronase (0.5% in HKSOM) digestion. Mathematical modeling of the gradients around embryos suggested that more reliable signals could be obtained at a distance of 6 μm away from embryos. Accordingly, all subsequent recordings were obtained at this standard distance. Data acquisition and manipulation were performed as described previously [19–22]. The hardware and software controlling electrode movements, signal amplification, and data acquisition were designed and constructed by the BioCurrents Research Center at the Marine Biological Laboratory, Woods Hole, MA (www.mbl.edu/BioCurrents [case sensitive]). The lower limit of detection, with a signal-to-noise ratio of three, was approximately a 0.01 μM difference in oxygen concentration between the two excursion points, and the oxygen signals we document here were greater than 10 times this lower detection limit. All data are presented as mean ± standard deviation unless otherwise specified.

Digital images of embryos were captured periodically throughout the experiment using a Cohu analog video camera (Cambridge Research Instruments, Cambridge, MA) and a personal computer running Metamorph Software (Universal Imaging Corp., West Chester, PA). The morphometric features of embryos were analyzed from these images using Metamorph Software.

Stock solutions of mitochondrial toxins, carbonyl cyanide *P*-trifluoro-methoxyphenyl-hydrazone (FCCP, 1 mM) and antimycin A (1 mM), were prepared in ethanol. On the day of use, these stocks were further diluted to a concentration of 100 μM in ethanol. Stock solutions of sodium cyanide (1 M) were prepared in water, daily. While recording oxygen gradients from embryos, stock solutions containing mitochondrial toxins were added to the physiological medium to yield the final desired concentrations: 1 μM FCCP, 1 μM antimycin A, 1 mM sodium cyanide, 0.01% solvent. Cyanide at 1 mM is more than adequate to inhibit mitochondrial cytochrome oxidase [31]. To induce disruption in mitochondria associated with cell death, one-cell embryos and blastocysts were treated with 50 μM diamide for 3 h, according to the procedures previously reported [23]. To investigate the influence of the metabolic substrate, pyruvate, on oxygen consumption, one-cell embryos, harvested 22–23 h after hCG injection (see below), were transferred into pyruvate-free KSOM 6–7 h after retrieval (28–29 h after hCG injection) and cultured overnight. Several hours after culture in pyruvate-free medium these embryos cleaved in a manner similar to control sibling embryos that were incubated in standard KSOM containing 0.2 mM pyruvate, and although the blastomeres were smaller (see *Results*) they were otherwise morphologically indistinguishable. Oxygen consumption measurements from the resulting two-cell embryos cultured overnight in pyruvate-free medium were conducted in HEPES-buffered pyruvate-free KSOM and in a similar manner as measurements from control embryos conducted in HEPES-buffered KSOM containing 0.2 mM pyruvate.

Female B6C3F1 mice (6 wk old) were purchased from Charles River (Boston, MA) and subjected to a 14L:10D cycle for at least 1 wk before use. Animals were cared for according to procedures approved by the Marine Bio-

logical Laboratory and Women and Infants Hospital Animal Care Committees. Male B6C3F1 mice of proven fertility were used for mating. Female mice were superovulated by intraperitoneal injection of 7.5 IU PMSG (Calbiochem, La Jolla, CA) followed 46–48 h later by injection of 7.5 IU hCG, and mated individually. Females exhibiting mating plugs were selected the next morning and killed by cervical dislocation at 22–23 h after hCG injection. Zygotes (~30/animal) enclosed in cumulus masses were released from the ampullae into HKSOM supplemented with 0.03% hyaluronidase. Cumulus cells were gently removed from one-cell embryos by pipetting. Cumulus-free one-cell embryos were washed in HEPES-buffered KSOM three times and then in pre-equilibrated modified KSOM three times. Modified KSOM used for in vitro culture was supplemented with nonessential amino acids (1 ml of 100× stock/100 ml medium) and 2.5 mM HEPES. Embryos were pooled, randomly distributed, and cultured in 50-μl droplets (7–16 embryos/drop) under mineral oil at 37°C in a humidified atmosphere of 7% CO_2 in air. These embryo harvest and in vitro culture procedures sustained development of control one-cell embryos to blastocysts (>90%) and subsequent development to term. For most experiments, the zona pellucida was removed mechanically following mild treatment with pronase. No difference in physiological signals was observed if the embryos were examined immediately following ZP removal or after a 0.5–2.5-h incubation/recovery period. Zona-free embryos cleaved in a manner similar to zona-intact sibling embryos. All reagents were purchased from Sigma Chemical Co. (St. Louis, MO), unless stated otherwise.

RESULTS

Oxygen Gradients Around Embryos

Using an oxygen-sensitive electrode in self-referencing mode, the concentration of dissolved oxygen in the medium surrounding individual mouse embryos could be measured reliably and was stable over the recording duration (~1 h). The dissolved oxygen concentration of the medium near one-cell embryos was reduced by 0.33 ± 0.07 μM relative that of the bulk medium (0.21 mM), such that a gradient of depleted dissolved oxygen surrounded each embryo (Fig. 1A). The concentration of oxygen in the medium was most depleted nearest the embryos and the medium was less depleted of oxygen with increasing distance from the embryo. The gradient of dissolved oxygen concentration could be measured >50 μm away from the embryo surface (Fig. 2).

The dissolved oxygen concentration nearest embryos of different developmental stages was characteristic of the particular stage and the medium surrounding later developmental stages was more depleted of oxygen than that surrounding earlier stages. On average, the medium near a two-cell embryo was more depleted of oxygen (0.43 ± 0.10 μM below that of the bulk medium, n = 22) than the medium surrounding a one-cell embryo (0.33 ± 0.07 μM below that of the bulk medium, n = 8) (Fig. 1B). However, the radius of a two-cell blastomere (26.9 ± 0.6 μm; n = 22) was less than that of a one-cell embryo (37.3 ± 0.7 μm; n = 16), and therefore, the position of the probe relative to the geometric center of the specimen was not equivalent between embryos of different developmental stages. A mathematical function was determined that allowed the oxygen gradients surrounding embryos of different sizes to be adjusted geometrically and thus compared quantitatively (Fig. 2B). The only assumption intrinsic to this function was that the oxygen consumption was relatively homogeneous around the embryo. Measurements from different locations around embryos have not revealed regional difference in oxygen gradients and thus experimentally confirmed this assumption. Perhaps surprisingly, oxygen consumption measurements around blastocysts also did not reveal regional differences (e.g., inner cell mass versus polar trophectoderm), and we are presently investigating whether the diffusional properties of oxygen underlie this signal normalization. A series of 120 measurements were obtained at various distances (>6 μm) from nine blastocysts, and a standard curve was generated with the function

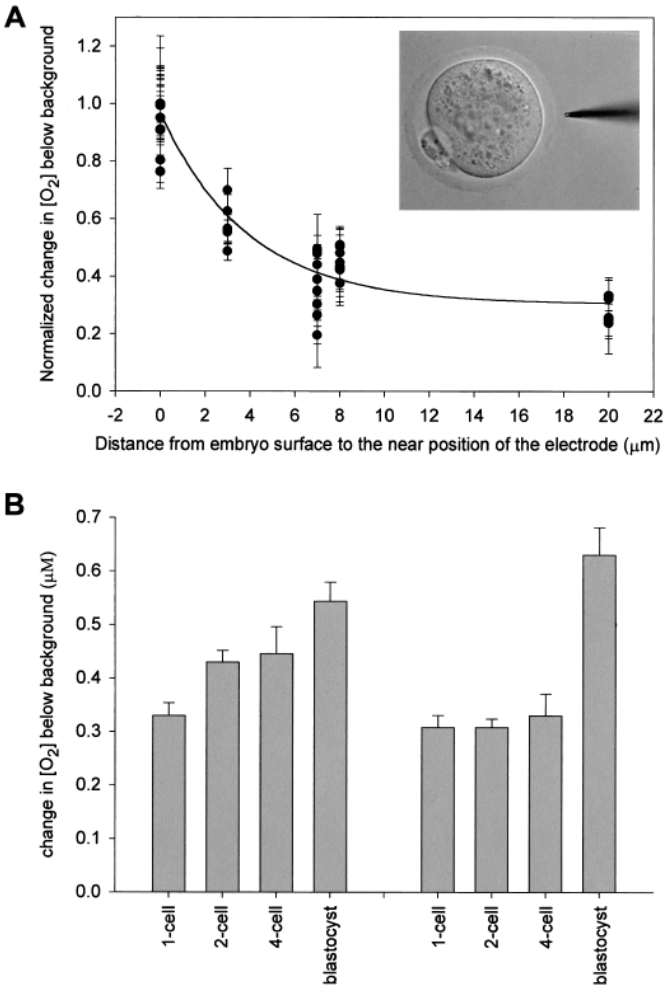

FIG. 1. Using a Whalen-type oxygen electrode in self-referencing mode, a gradient of dissolved oxygen could be measured around individual embryos. (**A**) The gradient of depleted oxygen extended tens of microns into the medium away from one-cell embryos (n = 7). The closest probe position (0) was 0.25–0.75 μm away from the zona pellucida surface. Each point is the mean ± standard deviation of >25 samples taken during a 3–5-min period of self-referencing with the electrode position nearest to the embryo plotted. (**Inset**) Image of a mouse one-cell embryo and juxtaposed oxygen electrode. (**B**) Different developmental stages depleted the surrounding medium of oxygen to different extents (n = 7–22 for each group). The concentration of oxygen in the medium nearest embryos became more depleted relative to the bulk medium (0.21 mM) as development progressed. Scaling of the data to account for variations in embryo size (see text) demonstrated that the medium surrounding blastocysts was twice as depleted of oxygen as that surrounding cleavage-stage embryos, suggesting at least a twofold increase in oxygen consumption by blastocysts. Data are presented as the change in dissolved oxygen concentration near embryos relative to that of the bulk medium (background = 0.21 mM).

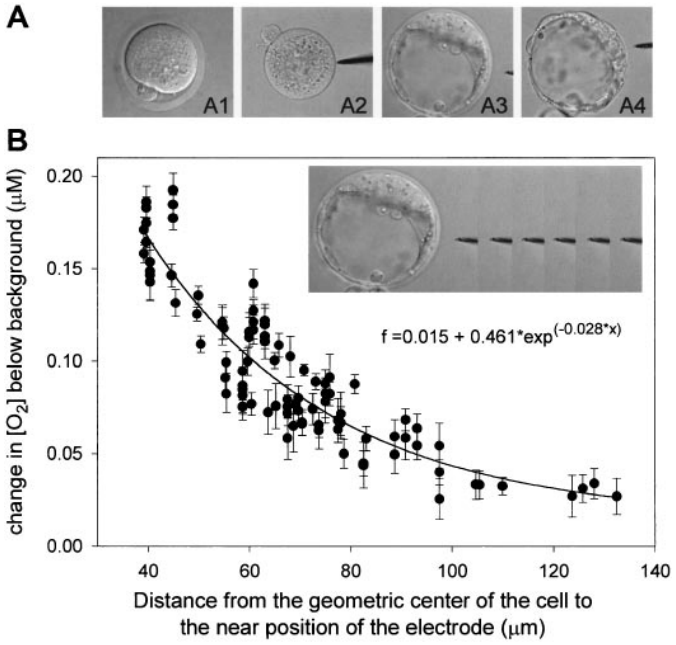

FIG. 2. Quantification of oxygen consumption by embryos that varied in size required a mathematical scaling function. (**A**) Embryos of different developmental stages exhibit significantly different radii. (**A1**) One-cell embryo, zona pellucida intact. (**A2**) One-cell embryo, zona pellucida remove. (**A3**) Blastocysts, zona pellucida intact. (**A4**) Blastocysts, zona pellucida removed. Removal of the zona did not alter the embryo morphology or the surrounding oxygen gradients. Dark point in A2–A4 was the oxygen-selective electrode. (**B**) A mathematical function was determined that allowed oxygen gradients surrounding embryos of different sizes to be adjusted geometrically and quantitatively compared. A series of 120 measurements were obtained at various distances (>6 μM) from nine blastocysts that ranged in radii from 32 to 62 μm, and a standard curve was fitted with the equation noted. Data presented as the change in dissolved oxygen concentration near embryos relative to that of the bulk medium (background = 0.2102 mM). Each point is the mean ± standard deviation of >25 samples taken during a 3–5-min period of self-referencing with the electrode position nearest to the embryo plotted as the distance from geometric center of the embryo. (**Inset**) Oxygen electrode at various distances from a blastocyst.

$$f = 0.015 + 0.461 \times e^{(-0.028 \times x)} \quad (1)$$

where x is the distance from the electrode tip to the geometric center of the cell as determined from images of embryos taken at an equatorial focal plane (Fig. 2B). Scaling to a common radius of 40 μm occurred by Eq. 2

$$\text{scaled } \Delta[O_2] = (\text{measured } \Delta[O_2]/[0.015 + 0.461 \times e^{(-0.028 \times x)}]) \times [0.015 + 0.461 \times e^{(-0.028 \times 40)}] \quad (2)$$

This set of equations has been verified in more than a dozen subsequent experiments from more than 80 embryos of a variety of developmental stages, including some devoid of their zona pellucida, and in each case the data could be fit with this function.

The mathematical function was used to normalize the oxygen concentration values obtained near embryos of different sizes and yielded the following relationships; all cleavage-stage embryos (one-, two-, and four-cell) depleted the surrounding medium of oxygen to a similar degree (change in dissolved $[O_2] = \sim 0.3$ μM below that of the bulk medium) and the medium surrounding blastocysts was depleted of oxygen twofold more than that surrounding cleavage-stage embryos (change in dissolved $[O_2] = 0.6 \pm 0.1$ μM below that of the bulk medium) (Fig. 1B).

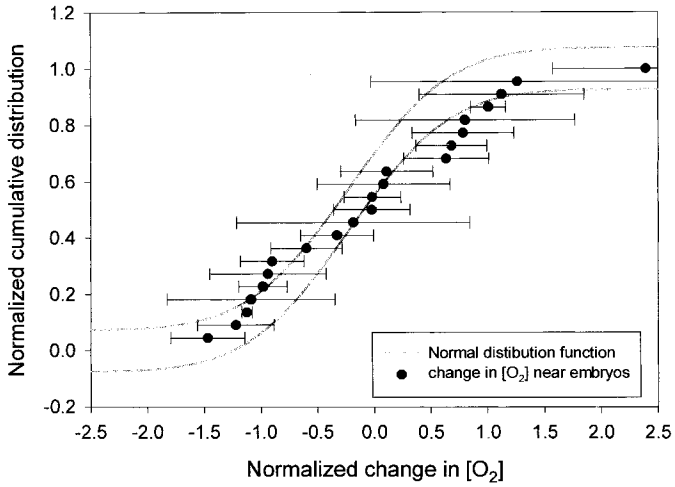

FIG. 3. Oxygen gradient measurements from a population of 22 two-cell embryos exhibited a normal distribution as evident by an overlap between the standard error bars for the normalized change in oxygen concentration surrounding each embryo and the 95% confidence intervals of a normal distribution function (gray lines) in a Kolmogorov-Smirnov plot. There appeared to be no obvious correlation between the magnitude of the oxygen gradient around an embryo and its developmental competence (see text).

These values highlight the sensitivity of the self-referencing electrode technique. The concentration of dissolved oxygen in bulk medium was 0.2102 mM, and the medium immediately surrounding individual blastocysts was depleted of oxygen such that the oxygen concentration declined to 0.2096 mM or a change of only 1/350th. Yet, the oxygen electrode in self-referencing mode could reliably and unequivocally detect this minute change in oxygen concentration.

It was likely that the region of depleted oxygen surrounding individual embryos resulted from oxygen consumption by the embryo, and oxygen consumption by individual embryos could be calculated using Fick's law: flux = oxygen diffusion coefficient × ($\Delta[O_2]$/probe excursion) [19–22]. The degree of oxygen depletion we observed around embryos corresponded to an oxygen consumption by individual cleavage-stage embryos of 7.7 pmol O_2 cm^{-2} h^{-1} (or 0.1 nl $embryo^{-1}$ h^{-1}) and by individual blastocysts of 15.8 pmol O_2 cm^{-2} h^{-1} (or 0.3 nl $embryo^{-1}$ h^{-1}).

Oxygen gradient measurements from 22 individual two-cell embryos exhibited a normal distribution with a median (±95% confidence intervals) of 0.31 ± 0.03 μM below that of the bulk medium and ranged from 0.27 to 0.41 μM below that of the bulk medium (Fig. 3). Subsequent to obtaining the oxygen measurements, 16 of these two-cell embryos were cultured and >90% developed to blastocysts. There appeared no obvious correlation between the magnitude of the oxygen gradient around an embryo and its developmental competence; however, almost all mouse embryos in this study exhibited robust development, thereby limiting the power of the analysis to determine a relationship between oxygen consumption and developmental potential. Present experiments employing other model systems continue to investigate this relationship (see *Diamide Oxidation Modulates Oxygen Consumption* below).

Oxygen Gradients Result, in Part, from Metabolic OXPHOS

The oxygen gradients surrounding embryos arose from a combination of mitochondrial OXPHOS and oxygen consumption by other oxygenases not associated with OXPHOS. To determine the proportion of the oxygen gradients resulting from OXPHOS, we measured oxygen gradients around individual embryos exposed to the following mitochondria uncouplers and toxins: FCCP that increases oxygen consumption by mitochondria through uncoupling the proton gradient from oxidative phosphorylation; sodium cyanide and antimycin A that reduce oxygen consumption by mitochondria through blocking electron flow at different sites within the oxidative phosphorylation cascade [31]. Embryos treated with FCCP (1 μM) consumed more oxygen as indicated by a greater depletion of oxygen from the surrounding medium (Fig. 4A,B). The medium surrounding individual one-cell embryos treated with FCCP was more depleted of oxygen (89.2 ± 31.2% more) compared to the baseline oxygen concentration prior to FCCP treatment (0% in Fig. 4B), indicating that the mitochondria of FCCP-treated embryos consumed more oxygen than did those of control cleavage-stage embryos (Fig. 4). Similarly, the medium surrounding individual blastocysts treated with FCCP was more depleted of oxygen than that surrounding control untreated blastocysts, but only 49.5 ± 25.9% more depleted than the baseline oxygen concentration prior to FCCP treatment (0% in Fig. 4B), indicating a relatively more modest increase of OXPHOS in blastocysts following FCCP treatment.

Both cyanide (1 mM) and antimycin A (1 μM) decreased oxygen consumption by embryos as observed by a return of the medium oxygen concentration near embryos toward concentrations more similar to that of the bulk medium (Fig. 4A,B). The medium surrounding individual two-cell embryos treated with cyanide or antimycin A was less depleted of oxygen (~23% less) than that surrounding control untreated embryos, indicating a decline in oxygen consumption by treated embryos (Fig. 4B). Expressed another way, ~77% of the oxygen consumed by cleavage-stage embryos was cyanide/antimycin A resistant. The medium surrounding individual blastocysts treated with cyanide or antimycin A was substantially less depleted of oxygen (60–70% less) than that surrounding control blastocysts, indicating that antimycin A and cyanide evoked a pronounced decrease in oxygen consumption by blastocysts (Fig. 4B). By contrast to cleavage-stage embryos, only ~30% of the oxygen consumed by blastocysts was cyanide/antimycin A resistant. These numbers could be used to calculate the contribution of OXPHOS-independent oxygen consumption to the total oxygen depleted from the surrounding medium and yielded an interesting result; the medium surrounding both cleavage-stage embryos and blastocysts was similarly depleted of 0.2 μM dissolved oxygen by OXPHOS-independent mechanisms. Therefore, OXPHOS-independent oxygen consumption remained relatively constant throughout embryo development, while mitochondrial OXPHOS-dependent oxygen consumption substantially increased between cleavage-stage embryos and blastocysts (Fig. 4C).

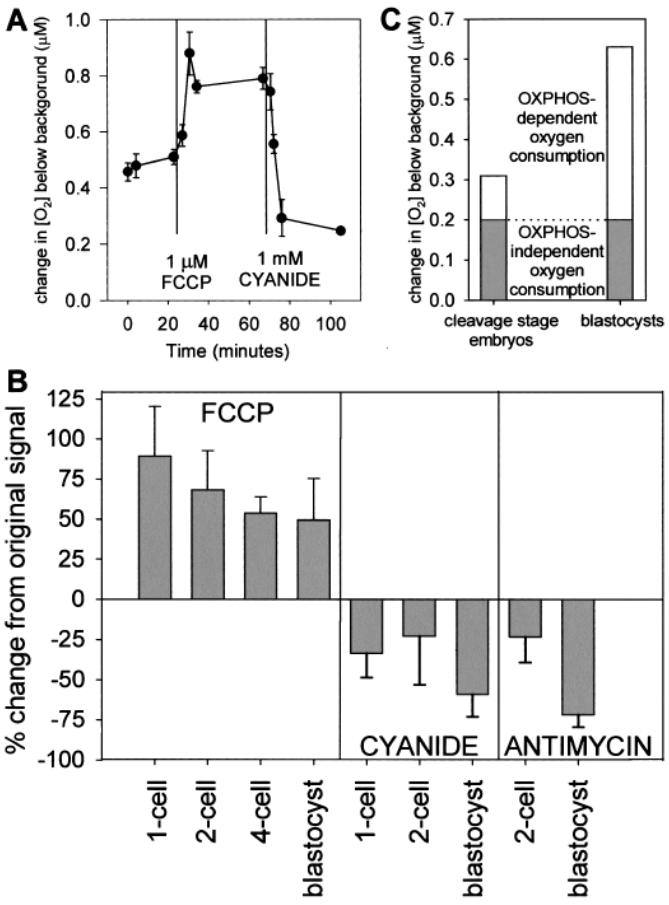

FIG. 4. Mitochondrial toxins modulated the oxygen consumed by embryos. (**A**) The FCCP (1 μM) rapidly increased and cyanide (1 mM) quickly decreased the oxygen consumed by an individual blastocyst as evident by alterations in the dissolved oxygen concentration in the surrounding medium relative to that of the bulk medium. Each point is the mean ± standard deviation of >25 samples taken during a 3–5-min period of self-referencing and plotted at the median sample time. (**B**) The FCCP (1 μM) increased oxygen consumption by cleavage-stage embryos and blastocysts. Cyanide (1 mM) and antimycin A (1 μM) greatly decreased oxygen consumption by blastocysts but only modestly decreased oxygen consumption by cleavage-stage embryos (single factor ANOVA, cyanide, $P < 0.03$; antimycin A, $P \ll 0.01$). Mean ± standard deviation; n = 22 FCCP-treated embryos with more than 4 embryos in each group, n = 15 cyanide-treated embryos with more than 4 embryos in each group n = 16 antimycin A-treated embryos with more than 6 embryos in each group. (**C**) Calculations of the contribution of OXPHOS-dependent and OXPHOS-independent oxygen consumption, based upon FCCP, cyanide, and antimycin A data. The majority of oxygen consumed by cleavage-stage embryos was not utilized by OXPHOS (OXPHOS-independent oxygen consumption), whereas the majority of oxygen consumed by blastocysts was utilized by OXPHOS (OXPHOS-dependent oxygen consumption). The OXPHOS-independent oxygen consumption remains relatively constant throughout development, while OXPHOS in blastocysts consumed six times more oxygen than did OXPHOS of cleavage-stage embryos. Data are presented as the change in the dissolved oxygen concentration near embryos relative to that of the bulk medium (background = 0.21 mM).

Medium Pyruvate Concentration Modulates Oxygen Consumption

Embryos cultured overnight from the late one-cell to the two-cell stage in pyruvate-free KSOM (pyruvate-free embryos), consumed less oxygen than did control embryos cultured overnight in the presence of 0.2 mM pyruvate (Fig. 5). The medium surrounding individual pyruvate-free, two-cell embryos was less depleted of oxygen than that surrounding control embryos (Fig. 5A). This difference in the degree of oxygen depletion was partially masked by the smaller size of pyruvate-free embryos (pyruvate-free embryo radii = 26.6 ± 0.9 μm; control embryo radii = 28.5 ± 0.7 μm; single factor ANOVA, $P \ll 0.005$) that allowed positioning of the electrode closer to the center of pyruvate-

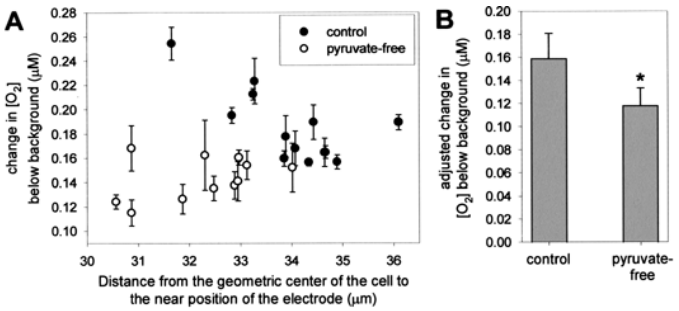

FIG. 5. Late one-cell embryos cultured overnight in pyruvate-free medium, cleaved to two cells but consumed less oxygen than did control embryos cultured in medium containing 0.2 mM pyruvate. Data are presented as the change in dissolved oxygen concentration near embryos relative to that of the bulk medium (background = 0.21 mM). (**A**) Unscaled data illustrating the relationship between, treatment, embryo size, and change in oxygen concentration of the medium near embryos. Each point is the mean ± standard deviation of >25 samples taken during a 3–5-min period of self-referencing with the electrode position nearest to the embryo plotted as the distance from the embryo center. Measurements were taken 6 μm away from the surface of embryos from which the zona had been removed (n = 11 pyruvate-free embryos, 13 control embryos). Pyruvate-free embryos were smaller and consumed less oxygen than did control embryos. (**B**) Scaling of data from A using the mathematical function described in the text demonstrated that control embryos depleted the surrounding medium of 26% more oxygen than did embryos cultured overnight in pyruvate-free medium (mean ± standard deviation; $P \ll 0.005$).

free embryos and thereby methodologically increased the signal (Fig. 5A). By using the mathematical function described earlier (Eqs. 1 and 2, Fig. 2B and associated text), the oxygen gradients around pyruvate-free and control embryos could be scaled such that embryos varying in size could be compared quantitatively. Upon scaling the average oxygen concentration of the medium surrounding pyruvate-free embryos was 0.12 ± 0.02 μM below that of the bulk medium, while the oxygen concentration of the medium surrounding control embryos was 0.16 ± 0.02 μM below that of the bulk medium (single factor ANOVA, $P \ll 0.005$) (Fig. 5B). Embryos cultured overnight in the absence of pyruvate consumed 26% less oxygen than those cultured in medium containing pyruvate.

Diamide Oxidation Modulates Oxygen Consumption

Diamide, a glutathione oxidizing agent, evokes changes in mitochondria associated with cell death in mammalian embryos [23]. Embryos treated with 50 μM diamide for 3 h consumed less oxygen than did untreated, control embryos (Fig. 6). The medium surrounding individual diamide-treated one-cell embryos was less depleted of oxygen than that surrounding control embryos (Fig. 6A). Scaling of these data using the mathematical function described earlier (Eqs. 1 and 2, Fig. 2B and associated text) allowed embryos varying in size, to be compared quantitatively. The medium surrounding diamide-treated one-cell embryos was less depleted of oxygen (0.12 ± 0.02 μM below that of the bulk medium) than that surrounding control one-cell embryos (0.18 ± 0.01 μM below that of the bulk medium) (single factor ANOVA, $P \ll 0.005$) (Fig. 6B). One-cell embryos

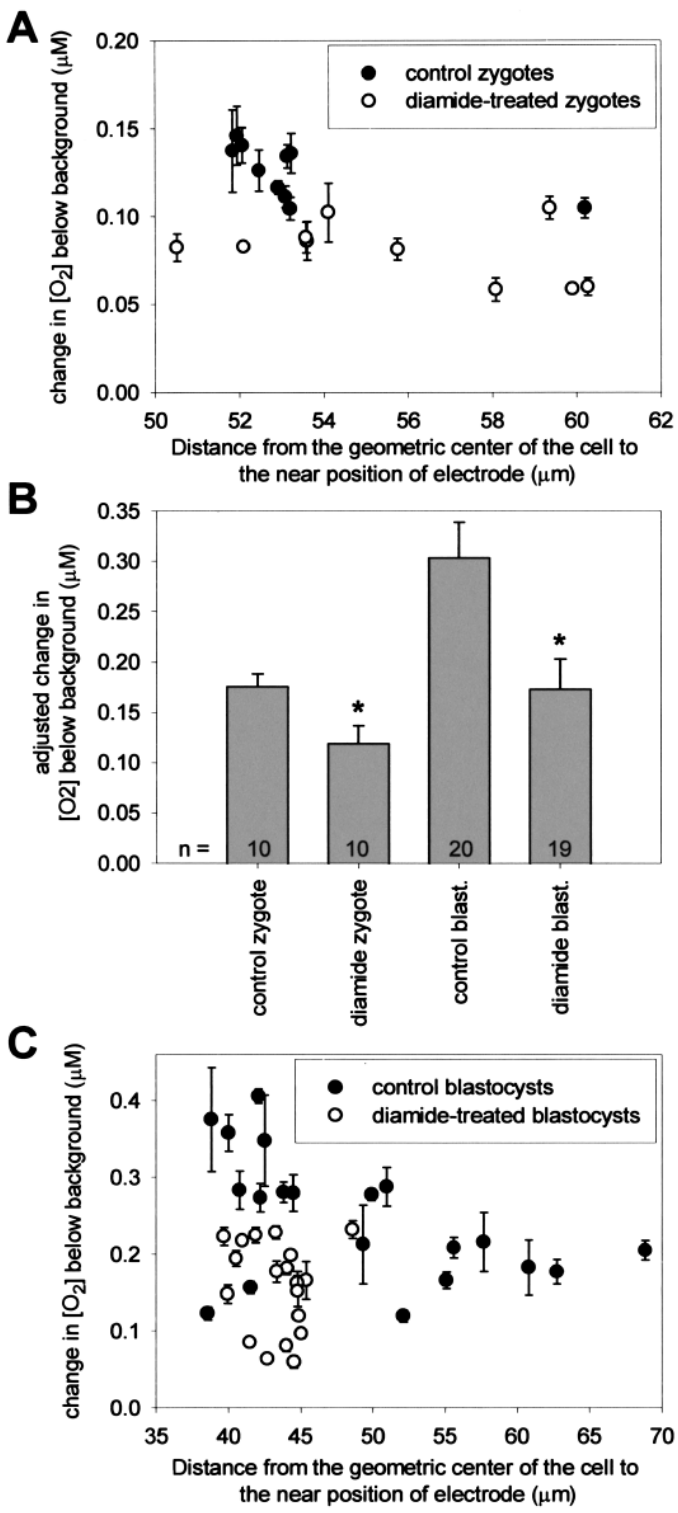

embryos relative to that of the bulk medium (background = 0.2102 mM). (**A,C**) Unscaled data illustrating the relationship between, treatment, embryo size, and change in oxygen concentration of the medium near embryos (A = one-cell embryos; C = blastocysts). Each point is the mean ± standard deviation of >25 samples taken during a 3–5-min period of self-referencing with the electrode position nearest to the embryo plotted as the distance from the embryo center. Measurements were taken 6 μm away from the surface of embryos from which the zona had been removed (n = 11 pyruvate-free embryos, 13 control embryos). Diamide-treated embryos were smaller and consumed less oxygen than did control embryos. (**B**) Scaling of data from A and C using the mathematical function described in the text demonstrated that dying embryos (50 μM diamide for 3 h) depleted the surrounding medium of less oxygen than did control embryos (mean ± standard deviation; $P \ll 0.005$).

FIG. 6. Embryos undergoing pharmacologically induced cell death (50 μM diamide for 3 h) consumed less oxygen than did control embryos. Data are presented as the change in dissolved oxygen concentration near

treated with diamide and undergoing cell death consumed 32% less oxygen than did control healthy embryos.

Similarly, the medium surrounding individual diamide-treated blastocysts was less depleted of oxygen than that surrounding untreated, control blastocysts (Fig. 6C). Upon mathematical scaling, the oxygen concentration of the medium surrounding diamide-treated blastocysts was substantially less depleted of oxygen (0.17 ± 0.03 μM below that of the bulk medium) than that surrounding control blastocysts (0.30 ± 0.04 μM below that of the bulk medium) (single factor ANOVA, $P \ll 0.005$) (Fig. 6B). Blastocysts treated with diamide consumed 43% less oxygen than do control blastocysts.

DISCUSSION

The self-referencing electrode technique was used to measure the amount of oxygen consumed by individual preimplantation embryos by noninvasively measuring the amount of oxygen depleted from the surrounding medium. A gradient of depleted dissolved oxygen surrounded each embryo and embryos had a profound influence on the concentration of available oxygen at distances of 50 μm and more from the embryo surface. This gradient of depleted oxygen extends away from the embryo into the adjacent medium to distances greater than one-half the embryo's diameter. Neighboring embryos communally cultured in a microdrop in vitro presumably could, therefore, influence the amount of oxygen available to each other. This physiological interaction between embryos may account, in part, for the enhanced cooperative development seen by groups of embryos cultured together versus embryos cultured singly [32, 33].

The measurements of oxygen consumption from individual embryos confirmed that blastocysts consume two to four times more oxygen than do cleavage-stage embryos [8–11, 18, 34]. More importantly, the oxygen consumed by embryos at different developmental stages contributed to different physiological processes. The portion of the total oxygen consumed by OXPHOS-dependent and OXPHOS-independent processes changed during preimplantation development [9, 11, 18, 34–36]. The majority (70%) of oxygen utilized by blastocysts was cyanide-sensitive [9, 16], consistent with oxygen utilization by OXPHOS within mitochondria. Benos and Balaban [16] suggested that 50–70% of all oxygen consumed by blastocyst-stage embryos was utilized by mitochondria to generate ATP for the Na/K-ATPase. Conversely, the minority (20–30%) of oxygen consumed by cleavage-stage embryos was cyanide sensitive, suggesting that OXPHOS-independent oxygenases contributed greatly to the total oxygen consumed by cleavage-stage embryos. Manes [37] suggested that a substantial portion of the OXPHOS-independent oxygen consumption by blastocysts contributes to surface H_2O_2 production and, indeed, Manes and Lai [17] determined that 30% of the total oxygen consumed by blastocysts was utilized by H_2O_2-producing oxygenases. Because cleavage-stage embryos produce only limited H_2O_2 [38] (unpublished observations), the two mixed multifunctional oxidase systems maturing in cleavage-stage embryos [38, 39] might account for the OXPHOS-independent oxygen consumption at this developmental stage.

In brief, we found, as did others [35, 36], that the OXPHOS-dependent/OXPHOS-independent ratio is approximately 30%/70% in cleavage-stage embryos and switches to 70%/30% in blastocysts. These ratios are compatible with data obtained from somatic cells [40, 41]. Cyanide-resistant oxygen consumption can contribute to between 10 and 90% of the total oxygen consumed by somatic cells and, in rare cases, such as during the burst of oxygen consumption that is characteristic of activated neutrophils, greater than 98% of the oxygen consumed is utilized by OXPHOS-independent oxygenases [40].

Although the estimations of OXPHOS-dependent/OXPHOS-independent ratios are based upon pharmacological manipulations, and therefore should be interpreted with caution, they are consistent with a host of other related changes that occur during preimplantation embryo development including: changes in mitochondria morphology from condensed structures in cleavage-stage embryos to swollen cristae-containing organelles in blastocysts [42–47]; an increase in mitochondria number in blastocysts resulting from mitochondria DNA and structural replication [44–49]; changes in the biogenesis of key OXPHOS enzymes [50, 51]; a decrease in total ATP content and ATP/ADP+P ratio that would stimulate OXPHOS [35, 52, 53]; and a change in energy substrate preferences and waste product secretion [18, 24, 25, 34–36, 54, 55].

By assimilating our findings with those of previous studies, a more complete picture of the developmental changes in energy metabolism emerges. At the two-cell stage, when the mitochondria are condensed, the total ATP content of the cell, as well as the ATP/ADP ratio are high, pyruvate is preferentially used as an energy substrate, lactate secretion is low, the total oxygen consumed and carbon dioxide produced is low, and OXPHOS-independent mechanisms account for the majority of oxygen consumed. At the blastocyst stage, when the mitochondria exhibit cristae, the total ATP content and the ATP/ADP ratio are low, stimulating aerobic glycolysis and OXPHOS-dependent mechanisms that increase lactate secretion, the total oxygen consumed, and carbon dioxide produced.

Despite the low levels of oxygen consumed by OXPHOS in cleavage-stage embryos, the self-referencing electrode technique could, nevertheless, detect changes in oxygen consumption resulting from alteration in the concentration of pyruvate in the medium. Pyruvate is preferentially utilized as an energy source by cleavage-stage embryos [9, 18, 25, 35, 36] and incubation of cleavage-stage embryos in medium devoid of pyruvate resulted in a decline in oxygen consumption by 26% ($P \ll 0.005$) over that consumed by control embryos [34]. This decline in total oxygen consumed was consistent with a decrease in mitochondrial oxygen consumption of ~90% and suggests that these cleavage-stage embryos did not appreciably compensate for the absence of pyruvate by utilizing other available metabolic substrates such as glucose (0.2 mM).

Finally, Magnusson et al. [12] suggested that human blastocysts that consumed more oxygen developed to blastocysts at higher rates than did those that consumed less oxygen. Independently, Overstrom et al. [15] confirmed this result using bovine blastocysts. Consistent with these findings, we demonstrate here that healthy control one-cell embryos and blastocysts consumed more oxygen than did those undergoing cell death. The early phases of cell death are associated with changes in mitochondria [23, 56, 57], and the change in oxygen consumption was detectable only 3 h after treatment with an agent (diamide) known to induce death of embryos [23]. These results suggest that changes in oxygen consumption might be indicative of disruptions in mitochondria and a decline in developmental competence. Future studies to investigate this relationship directly should now be possible by employing the self-referencing

electrode technique to monitor oxygen consumption from individual preimplantation embryos.

ACKNOWLEDGMENTS

We thank Richard Sanger and Katherine Hammer for assistance with the self-referencing technique and Gaudenz Danuser for his programming assistance and intellectual support.

REFERENCES

1. Pikó L, Matsumoto L. Number of mitochondria and some properties of mitochondrial DNA in the mouse egg. Dev Biol 1976; 49:1–10.
2. Jansen RP, de Boer K. The bottleneck: mitochondrial imperatives in oogenesis and ovarian follicular fate. Mol Cell Endocrinol 1998; 145: 81–88.
3. Taanman JW. The mitochondrial genome: structure, transcription, translation and replication. Biochim Biophys Acta 1999; 1410:103–123.
4. Kowaltowski AJ, Vercesi AE. Mitochondrial damage induced by conditions of oxidative stress. Free Radical Biol Med 1999; 26:463–471.
5. Barritt JA, Brenner CA, Cohen J, Matt DW. Mitochondrial DNA rearrangements in human oocytes and embryos. Mol Hum Reprod 1999; 5:927–933.
6. Dragiou I, Benetato G, Opreanu R. Recherches sur la respiration des ovocytes des mammiféres. C R Soc Biol 1937; 126:1044–1046.
7. Boell EJ, Needham J. Morphogenesis and metabolism: studies with the cartesian diver apparatus. I, II, III, IV. Proc R Soc Lond (B) 1939; 127:322–387.
8. Boell EJ, Nicholas JS. Respiratory metabolism of mammalian eggs and embryos. Anat Rec 1939; 75(suppl):66.
9. Fridhandler I, Hafez ESE, Pincus G. Developmental changes in the respiratory activity of rabbit ova. Exp Cell Res 1957; 13:132–139.
10. Boell EJ, Nicholas JS. Respiratory metabolism of the mammalian egg. J Exp Zool 1948; 109:267–281.
11. Mills RM, Brinster RL. Oxygen consumption of preimplantation mouse embryos. Exp Cell Res 1967; 47:337–344.
12. Magnusson C, Hillensjö T, Hamberger L, Nillson L. Oxygen consumption by human oocytes and blastocysts grown in vitro. Hum Reprod 1986; 1:183–184.
13. Magnusson C, Hillensjö T, Tsafriri A, Hultborn R, Ahrén K. Oxygen consumption of maturing rat ovaries. Biol Reprod 1977; 17:9–15.
14. Nilsson BO, Magnusson C, Widéhn S, Hillensjö T. Correlation between blastocysts oxygen consumption and trophoblast cytochrome oxidase reaction and initiation of implantation of delayed mouse blastocysts. J Embryol Exp Morphol 1982; 71:75–82.
15. Overstrom EW, Duby RT, Dobrinsky J, Roche JF, Boland MP. Viability and oxidative metabolism of the bovine blastocyst. Theriogenology 1992; 37:269.
16. Benos DJ, Balaban RS. Energy requirements of the developing mammalian blastocyst for active ion transport. Biol Reprod 1980; 23:941–947.
17. Manes C, Lai NC. Nonmitochondrial oxygen utilization by rabbit blastocysts and surface production of superoxide radicals. J Reprod Fertil 1995; 104:69–75.
18. Houghton FD, Thompson JG, Kennedy CJ, Leese HJ. Oxygen consumption and energy metabolism of the early mouse embryo. Mol Reprod Dev 1996; 44:476–485.
19. Smith PJS. The non-invasive probes—tools for measuring transmembrane ion flux. Nature 1995; 378:645–646.
20. Smith PJS, Hammar K, Porterfield DM, Sanger RH, Trimarchi JR. A self-referencing, non-invasive, ion-selective electrode for single cell detection of trans-plasma membrane calcium flux. Microsc Res Tech 1999; 46:398–417.
21. Land SC, Porterfield DM, Sanger RH, Smith PJS. The self-referencing oxygen-selective microelectrode: detection of transmembrane oxygen flux from single cells. J Exp Biol 1999; 202:211–218.
22. Porterfield DM, Trimarchi JR, Keefe DL, Smith PJS. Characterization of oxygen and calcium fluxes from early mouse embryos and oocytes. Biol Bull 1998; 195:208–209.
23. Liu L, Trimarchi JR, Keefe DL. Thiol oxidation-induced embryonic cell death in mice is prevented by the antioxidant dithiothreitol. Biol Reprod 1999; 61:1162–1169.
24. Lane M, Gardner DK. Selection of viable mouse blastocysts prior to transfer using metabolic criterion. Hum Reprod 1996; 11:1975–1996.
25. Gott AL, Hardy K, Winston RM, Leese HJ. Non-invasive measurement of pyruvate and glucose uptake and lactate production by single human preimplantation embryos. Hum Reprod 1990; 5:104–108.
26. Wokosin DL, White JG, Bavister BD, Squirrell JM. Long-term two-photon fluorescence imaging of mammalian embryos without compromising viability. Nat Biotechnol 1999; 17:763–767.
27. Ray PF, Ao A, Taylor DM, Winston RM, Handyside AH. Assessment of the reliability of single blastomere analysis for preimplantation diagnosis of the delta F508 deletion causing cystic fibrosis in clinical practice. Prenatal Diagn 1998; 18:1402–1412.
28. Muggleton-Harris AL, Glazier AM, Pickering S, Wall M. Genetic diagnosis using polymerase chain reaction and fluorescent in-situ hybridization analysis of biopsied cells from both the cleavage and blastocyst stages of individual cultured human preimplantation embryos. Hum Reprod 1995; 10:183–192.
29. Emmanouilidou E, Teschemacher AG, Pouli AE, Nicholls LI, Seward EP, Rutter GA. Imaging Ca(2+) concentration changes at the secretory vesicle surface with a recombinant targeted cameleon. Curr Biol 1999; 9:915–918.
30. Pollok BA, Heim R. Using GFP in FRET-based applications. Trends Cell Biol 1999; 9:57–60.
31. Stryer L. Biochemistry. New York: WH Freeman and Co; 1988.
32. Moessner J, Dodson WC. The quality of human embryo growth is improved when embryos are cultured in groups rather than separately. Fertil Steril 1995; 64:1034–1035.
33. Gardner DK, Lane MW, Lane M. Development of the inner cell mass in mouse blastocysts is stimulated by reducing the embryo:incubation volume ratio. Hum Reprod 1997: 12:182–183.
34. Fridhandler L. Pathways of glucose metabolism in fertilized rabbit ova at various pre-implantation stages. Exp Cell Res 1961; 22:303–316.
35. Biggers JD, Borland RM. Physiological aspects of growth and development of the preimplantation embryo. Annu Rev Physiol 1976; 38: 95–119.
36. Leese HJ. Metabolic control during preimplantation mammalian development. Hum Reprod Update 1995; 1:63–72.
37. Manes C. Cyanide-resistant reduction of nitroblue tetrazolium and hydrogen peroxide production by the rabbit blastocyst. Mol Reprod Dev 1992; 31:114–121.
38. Balling R, Haaf H, Maydl R, Metzler M, Beier HM. Oxidative and conjugative metabolism of diethylstilbestrol by rabbit preimplantation embryos. Dev Biol 1985; 109:370–374.
39. Filler R, Lew KJ. Developmental onset of mixed function oxidase activity in preimplantation embryos. Proc Natl Acad Sci USA 1981; 78:6991–6995.
40. Curnutte JT, Babior BM. Chronic granulomatous disease. Adv Hum Genet 1987; 16:229–297.
41. Kumar S, Acharya Kumar S. 2,6-Dichloro-phenol indophenol prevents switch-over of electrons between the cyanide-sensitive and -insensitive pathway of the mitochondrial electron transport chain in the presence of inhibitors. Anal Biochem 1999; 268:89–93.
42. Mackler B, Grace R, Haynes B, Bargman GJ, Shepard TH. Studies of mitochondrial energy systems during embryogenesis in the rat. Arch Biochem Biophys 1973; 158:885–888.
43. Shepard TH, Muffley LA, Smith LT. Ultrastructural study of mitochondria and their cristae on embryonic rats and primates (*N. nemistrina*). Anat Rec 1998; 252:383–392.
44. Hillman N, Tasca R. Ultrastructural autoradiographic studies of mouse cleavage stages. Am J Anat 1969; 126:151–174.
45. Stern S, Biggers J, Anderson E. Mitochondria and early development of the mouse. J Exp Zool 1971; 176:179–192.
46. Calarco PG, Brow EH. An untrastructural and cytological study of preimplantation development of the mouse. J Exp Zool 1969; 171: 253–283.
47. Chech S, Sedlácková M. Ultrastructure and morphometric analysis of preimplantaiton mouse embryos. Cell Tissue Res 1983; 230:661–670.
48. Pikó L. Synthesis of macromolecules in early mouse embryos cultured in vitro: RNA, DNA, and polysaccharide component. Dev Biol 1970; 21:257–279.
49. Pikó L, Chase DG. Role of the mitochondrial genome during early development in mice. Effects of ethidium bromide and chloramphenicol. J Cell Biol 1973; 58:357–378.
50. Taylor KD, Pikó L. Mitochondrial biogenesis in early mouse embryos: expression of the mRNAs for subunits IV, Vb, and VIIc of cytochrome C oxidase and subunit 9 (PI) of H+-ATP synthase. Mol Reprod Dev 1995; 40:29–35.
51. Pikó L, Taylor KD. Amounts of mitochondrial DNA and abundance of some mitochondrial gene transcripts in early mouse embryos. Dev Biol 1976; 123:364–374.

52. Ginsberg L, Hillman N. Shifts in ATP synthesis during preimplantation stages of mouse embryos. J Reprod Fertil 1975; 43:83–90.
53. Ginsberg L, Hillman N. ATP metabolism in cleavage-staged mouse embryos. J Embryol Exp Morphol 1973; 30:267–282.
54. Brinster RL. Carbon dioxide production from glucose by the preimplantation mouse embryo. Exp Cell Res 1967; 47:271–277.
55. Gardner DK, Lane M. Culture of viable human blastocysts in defined sequential serum-free media. Hum Reprod 1998; 13(suppl):148–159.
56. Crompton M. The mitochondria permeability transition pore and its role in cell death. Biochem J 1999; 341:233–249.
57. Gross A, McDonnell JM, Korsmeyer SJ. BCL-2 family members and the mitochondria in apoptosis. Genes Dev 1999; 13:1899–1911.